ADVANCED ENGINEERING MATERIALS
www.aem-journal.com

Research for the Safe Management of Nuclear Waste at Forschungszentrum Jülich: Materials Chemistry and Solid Solution Aspects

Dirk Bosbach, Felix Brandt, Andrey Bukaemskiy, Guido Deissmann, Philip Kegler, Martina Klinkenberg, Piotr M. Kowalski, Giuseppe Modolo, Irmgard Niemeyer, Stefan Neumeier, and Victor Vinograd*

The safe management of high-level nuclear wastes, including their final disposal in a deep geological repository, requires a sound scientific understanding of the processes affecting the various materials present in the multibarrier system of the disposal facility, including the radioactive waste forms. Thus materials science aspects play an important role in the multidisciplinary and complex field of long-term safety assessments. As many of these issues are related to mixed solid compounds, the aspect of structural radionuclide uptake by a host structure and subsequent solid solution formation is one of the key topics of the research related to nuclear waste management at Forschungszentrum Jülich. The adopted practice for deriving an in-depth understanding of materials behavior by combining state-of-the-art experimental and computational approaches is presented in the context of three examples: 1) corrosion of spent nuclear fuels, 2) radionuclide retention by secondary phases, and 3) innovative ceramic waste forms. New nano- and microanalytical tools, as well as advanced spectroscopic techniques and computational methods, further developed and tailored at Forschungszentrum Jülich, allowed for refined views on these materials.

1. Introduction

The safe management of radioactive wastes arising from electricity production from nuclear energy, including its ultimate disposal in a deep geological disposal facility, is one of the grand challenges of our times, especially for countries with large nuclear programs. Radioactive wastes arise throughout all stages of the nuclear fuel cycle as well as from a variety of other sources such as industrial and medical applications of radioisotopes and research or in industries handling and processing naturally occurring radioactive materials (NORM). High-level radioactive wastes (HLW) related to the nuclear electricity production include spent nuclear fuels (SNF) from nuclear power plants (i.e., in open "once-through" fuel cycles), waste streams from spent fuel reprocessing (i.e., nuclear waste glasses, compacted metallic wastes, etc.), and materials separated in the course of reprocessing (e.g., separated civilian plutonium).

The disposal of HLW from nuclear power generation faces major scientific and social challenges to demonstrate the long-term safety of the disposed nuclear materials to protect humans and the environment against dangers arising from ionizing radiation. The safe disposal of radioactive waste requires its isolation from the geo/biosphere until radioactive decay has reduced its radiotoxicity to innocuous levels. Based on several decades of research, development, and demonstration (RD&D) it is generally accepted at the technical and scientific level that disposal in mined deep geological repositories (i.e., at depth exceeding 500 m below ground level) is the safest and most sustainable option for the management of HLW, such as SNF—if considered as waste—or wastes resulting from SNF reprocessing.[1,2]

This article provides an overview on specific RD&D related to the scientific basis of the safety case for deep geological disposal of high-level nuclear wastes, performed at Forschungszentrum Jülich, focusing on materials science aspects. The examples detailed comprise the evaluation of the long-term corrosion behavior of SNF in a geological repository, the retention of safety-relevant radionuclides in the repository near field, and the assessment of the performance of tailor-made ceramic waste forms for specific waste streams (e.g., separated plutonium) under postclosure disposal conditions. Specific features of the pursued research approach on materials relevant for the safe management of nuclear wastes comprise 1) complementary

Prof. D. Bosbach, Dr. F. Brandt, Dr. A. Bukaemskiy, Dr. G. Deissmann, Dr. P. Kegler, Dr. M. Klinkenberg, Dr. P. M. Kowalski, Prof. G. Modolo, Dr. I. Niemeyer, Dr. S. Neumeier, Dr. V. Vinograd
Institute of Energy and Climate Research (IEK-6): Nuclear Waste Management and Reactor Safety
Forschungszentrum Jülich GmbH
Jülich 52425, Germany
E-mail: d.bosbach@fz-juelich.de

The ORCID identification number(s) for the author(s) of this article can be found under https://doi.org/10.1002/adem.201901417.

DOI: 10.1002/adem.201901417

experiments and advanced simulations (e.g., atomistic and quantum chemical simulations, nuclear simulations, cross-scale reactive transport simulations, etc.) using high-performance computing and data science approaches, 2) use of micronized radioactive sample materials for facilitation of experiments, and 3) application of state-of-the-art microscopic and (micro) spectroscopic methods. As solid solutions are intrinsic constituents of various components of a repository system, from the waste form (e.g., uranium oxide (UO_2) and mixed uranium–plutonium oxide (MOX; $(U,Pu)O_2$) SNF) and engineered barrier materials (e.g., bentonite or calcium–silicate–hydrate (C–S–H) phases in cementitious barriers) to minerals in the geosphere, a sound understanding of the thermodynamics and kinetics of solid solution systems is an integral component of this research.

The long-term isolation and containment of the radioactive wastes in a geological disposal facility is achieved through a multiple barrier system, combining man-made engineered barriers, comprising durable waste forms, corrosion-resistant waste containers as well as buffer and backfill materials, with a suitable geological barrier, the repository host rock. The selected geological formations envisaged for geological disposal of HLW vary among countries, but the main options are crystalline rocks (e.g., granite), clays and clay rocks, and salt rocks. **Table 1** summarizes key features and the materials used in some concepts for deep geological disposal of HLW.

The HLW/SNF containers emplaced in deep geological repositories built in clay formations or crystalline rocks will inevitably come into contact with groundwater after the closure of the repository. Even for repositories in salt rocks, the presence of water cannot be completely ruled out for less probable scenarios, for example, early failure of shaft seals and plugs. As a consequence, after container failure due to aqueous corrosion, radionuclides can be released from degrading waste forms and subsequently migrate into the geo/biosphere via the water pathway. Thus a fundamental mechanistic understanding of the processes governing 1) the long-term evolution of the materials present in the repository system, 2) the dissolution of the waste matrices and the associated release of radionuclides (radionuclide source term), and 3) the migration behavior of radionuclides in the near and far field and their potential retention in newly formed solids in the repository near field (so called secondary phases) on a molecular level is necessary to demonstrate and substantiate the long-term safety of the repository for the required timescales of up to one million years.

Dirk Bosbach is director of the Institute of Energy and Climate Research at Forschungszentrum Jülich, responsible for the research related to the safe management of nuclear waste and professor for nuclear waste management at RWTH Aachen University. He is the spokesperson of the research program NUSAFE within the German Helmholtz Association. He has a scientific background in mineralogy and radiochemistry. His scientific approach integrates experiment and simulation on topics related to nuclear materials and the behavior of radionuclides in the context of waste management.

2. Importance of Solid Solutions in Nuclear Waste Disposal

Many materials relevant for the management of nuclear wastes are not pure substances but solid solutions, existing over a range of chemical compositions. Radionuclide-containing solid solutions relevant to the deep-geological disposal of HLW include 1) primary phases (waste forms): spent nuclear fuel, borosilicate glass, single phase/multiple phase ceramics; and 2) secondary (alteration) phases which form during the long-term evolution of such a repository system (waste forms and near-field barrier components): alteration phases of waste form corrosion, iron (container) corrosion phases (green rust, magnetite) and cement phases (e.g., C–S–H).

Substitutional solid solutions form by the replacement of one atom by another atom. A disordered arrangement of different atoms over the same lattice is stabilized by the entropy. The size and charge difference of the substituting atoms and the flexibility of the host structure, e.g., its Young´s modulus, determine

Table 1. Characteristics of selected disposal systems for SNF and vitrified HLW.[3–5]

Country	Waste	Host rock	Buffer-material	Container material
Belgium	HLW/SNF	Clay (boom clay)	Cementitious	C-steel/concrete
Canada	SNF	Granite or sedimentary rocks	Bentonite	Cu/C-steel
Finland	SNF	Granite	Bentonite	Cu/cast iron
France	HLW/SNF	Clay (Callovo-Oxfordian)		C-steel
Germany	HLW/SNF	Granite/clay/salt	Not decided	Not decided
Japan	HLW	Generic	Bentonite	C-steel
Spain	HLW/SNF	Granite/clay	Bentonite	C-steel
Sweden	SNF	Granite	Bentonite	Cu/cast iron
Switzerland	HLW/SNF	Clay (Opalinus Clay)	Bentonite	C-steel
UK	HLW (SNF)	Generic	Bentonite	C-steel; Cu
USA	SNF/HLW	Tuff (unsaturated)	Bentonite	Ni–Cr, Ti drip shields

the extent of solid solution formation. In general, the chemical composition of a mixed phase is specified in terms of fixed end-member compositions—e.g., the binary solid solution $U_{1-x}Pu_xO_2$ can exist in a range of compositions specified by the mole fraction, x, of the end-member PuO_2. Solid solution formation is typically favored between isostructural end members, where the exchangeable atoms have the same charge and similar ionic radii. In many systems the mixing is incomplete. In general, solid solution formation is limited at low temperatures and is favored at higher temperatures.

Ceramic waste forms benefit from an extensive solid solution formation favoring large loads of incorporated radionuclides. However, even a limited concentration of an extra component could be useful. For example, the mechanical strength and thermal conductivity of UO_2-based nuclear fuel depend on trace level concentrations of Cr.[6] An incorporation of cations and/or anions whose charges deviate from the charges of anions and cations in a host end-member typically occurs along a coupled substitution scheme.

2.1. Thermodynamic Aspects

To describe the thermodynamic stability of solid solutions, certain thermodynamic functions need to be defined, namely, the configurational entropy and the enthalpy of mixing, which both contribute to the Gibbs free energy of mixing. The simplest level of theory corresponds to the so-called regular solid solution model, which implies a random distribution of the substituting atoms and a one-parameter equation to describe the enthalpy of mixing

$$\Delta H_{\text{mix}} = x(1-x)W \tag{1}$$

where x is the mole fraction of an arbitrarily chosen end member. The knowledge of the regular mixing parameter W (dimensionless form: $a_0 = W/(RT_0)$, $T_0 = 298.15$ K) allows for the calculation of the thermodynamic activities of the end members AL and BL in an $A_{1-x}B_xL$ solid solution, which are indispensable for the description of thermodynamic equilibria in solid solution–aqueous solution (SS–AS) systems, i.e., $A_{1-x}B_xL + H_2O$.[7]

In SS–AS systems, the commonly known concept of the aqueous solubility product needs an important extension. In contrast to pure phases, where the aqueous solubility is independent of the amount of solid present, the solubility of a solid solution phase depends on the molar ratios and the solubilities of the end members. Such a relationship is often visualized with so-called Lippmann diagrams.[7] **Figure 1** shows a Lippmann diagram of the (Ba, Ra)SO_4 system, illustrating the effects of different solubilities of the end members $BaSO_4$ and $RaSO_4$ and of varying the regular mixing interaction parameter.

Another important aspect that reveals itself in SS–AS equilibria is the dependence of the partitioning of a radionuclide between solid and aqueous phases on the total fraction of the radionuclide component in the system. Generally, the aqueous activity of a radionuclide species decreases proportionally to its mole fraction in the system. This is because the small mole fraction in the system determines the final dilute composition of the minority component in a solid solution phase and this, in turn, determines reduced activities of the corresponding

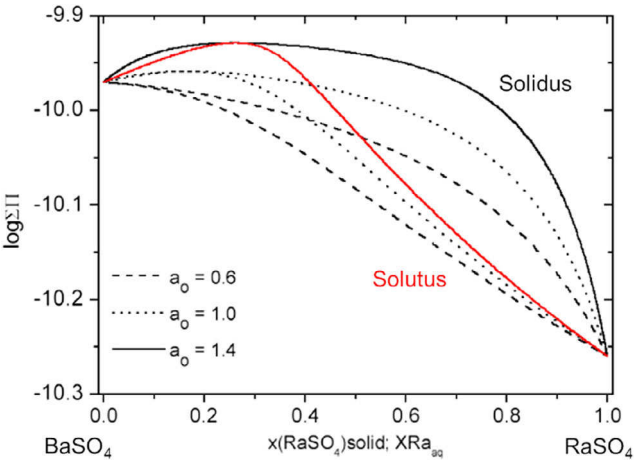

Figure 1. Example of a Lippmann diagram illustrating effects of different solubilities of end members and of the interaction parameter a_0. Calculated based on log $K^0_{BaSO_4} = -9.97$ and log $K^0_{RaSO_4} = -10.26$. The equilibrium composition of the aqueous phase in equilibrium with a solid of a given composition can be obtained by drawing a horizontal line connecting the solidus and solutus lines. Reproduced with permission.[8] Copyright 2013, Elsevier.

dissolved radionuclide species in the aqueous phase. In the case of full equilibration of an aqueous solution with a solid solution phase, in which a radionuclide is present in trace amounts, the solubility of the radionuclide in the aqueous solution can be reduced by orders of magnitude. Therefore, in some cases, solid solution formation can be a highly relevant process for the safety assessment, depending on the scenario.[9,10]

In many cases, only a partial equilibration of SS–AS systems is observed. This is revealed, for example, as sector and/or oscillatory compositional zoning.[11] Once a solid solution containing a certain nonequilibrium concentration of a radionuclide is precipitated from a supersaturated aqueous solution, a re-equilibration via solid state diffusion is practically impossible at temperatures below about 100 °C. However, some SS–AS systems could still evolve toward equilibrium via a dissolution reprecipitation process. In such cases, structural uptake of radionuclides from aqueous solutions is feasible with an effect of a significant decrease in aqueous radionuclide concentrations.

2.2. Experimental Approaches at Forschungszentrum Jülich

In recent years, new microscopic and spectroscopic instruments were set up in the Helmholtz Nano Facility (HNF) as well as at the Ernst Ruska-Centre for Microscopy and Spectroscopy with Electrons (ER-C) and the Central Institute of Analytics (ZEA-3) at Forschungszentrum Jülich. Complementarily, a new focused ion beam (FIB) instrument was installed in the radiochemistry laboratories of the Institute of Energy and Climate Research (IEK) of the Forschungszentrum Jülich, enabling the preparation of micronized samples from radioactive materials, e.g., tips for atom probe tomography (APT) or lamellae for high-resolution transmission electron microscopy (HRTEM). The advantage of sample micronization is the reduction of the radioactivity to levels below the exemption limit. This enabled the combination of

classical wet chemical experiments, ceramic synthesis, and other preparation techniques with state-of-the-art microanalyses. For example, the uptake of ^{226}Ra was observed in classical batch-type experiments and the solids were subsequently characterized in depth via HRTEM and APT, as well as time-of-flight secondary mass spectrometry (ToF-SIMS) (cf. Section 3.2).

2.3. Computational Approaches at Forschungszentrum Jülich

New computational approaches combined with the availability of high-performance supercomputing have recently paved the way for groundbreaking results regarding solid solution formation and the computation of such systems with quantum chemical methods—also for actinide elements with their highly correlated 5f electrons.

The determination of mixing properties of solid solutions from ab initio methods is a challenging task when it is performed via sampling and averaging over a plethora of polyatomic supercell configurations. The approach followed here consists in the notion that the configurational variability is greatly reduced in the dilute limit, whereas the thermodynamically useful properties can still be determined. Particularly, the regular mixing interaction parameter, W, whose importance for the thermodynamics of SS–AS systems is briefly discussed earlier, could be relatively easily derived from first principles via the so-called single defect method, by computing the increase in the total energy of a supercell of a host end member due to an insertion of a single substitutional defect corresponding to a dopant compound.[12] Calculations along the single defect methodology (SDM) were successfully performed for binary systems within the ternary (Ba, Sr, Ra)SO_4 barite-type sulfates, for ternary orthorhombic carbonates, (Ca, Sr, Ba)CO_3,[8] and for $La_{1-x}Ln_xPO_4$ (Ln = Ce, ..., Tb) and $La_{1-x}An_xPO_4$ (An = Pu, Am, Cm) monazite-type solid solutions.[13]

The next level of sophistication in this approach to solid solutions consists in the consideration of increments in the total energy of a host supercell from paired (double) substitutional defects. From these increments, one derives pairwise ordering interaction energies, through which temperature-dependent Gibbs free energies of mixing are computed reflecting effects of short- and long-range ordering. Calculations along the double-defect method (DDM) have been applied to all binary solid solutions systems within ternary (Ba, Sr, Ra)SO_4 barite-type sulfates, allowing for a detailed mapping of the ternary miscibility gap.[14]

A very important aspect of first-principles-based atomistic simulations of structural or thermodynamic parameters of materials, including solid solutions, is the use of proper and accurate computational methods. Many relevant radioactive elements contain strongly correlated d and f electrons and are thus challenging to first-principles-based computational methods, including density functional theory (DFT)—a workhorse of current computational chemistry and materials science. As an example, DFT fails to predict the semiconducting state for UO_2 (e.g., present in SNF), instead describing it as a metal.[15,16] Thus, feasible extensions of DFT such as DFT + U with the Hubbard U parameter derived from first principles were developed and extensively tested.[16–19] It was found that this approach significantly improves the prediction of structural and thermodynamic parameters of lanthanide phosphates and actinide-bearing molecular and solid compounds.[17,19,20] This method has been applied also to explain various properties and parameters of materials, such as their structural[17,21] and thermodynamic parameters,[22] their relative stability,[23,24] their electronic structure and X-ray absorption near edge structure (XANES) signatures,[25] and their defect formation energies.[26,27] It was also applied to derive reliable force fields for large-scale simulations of radiation damage processes[28] and to test the performance of different computational approaches for d and f electrons,[20] including advanced methodologies for computing solid solutions.[29,30]

3. Materials Research for Nuclear Waste Management in Jülich

3.1. Safety of Spent Nuclear Fuel Disposal

Nuclear fuel for most commercially used nuclear power reactors is based on ceramic uranium oxide (UO_2), or MOX containing the fissile isotopes ^{235}U and/or ^{239}Pu, in the form of pellets inserted in a cladding material (made in particular from zirconium alloys), forming a fuel rod. In addition to these commercial fuels from power reactors, a variety of nonconventional fuels from research reactors and prototype/test reactors exist. The fuel of so-called pebble-bed high-temperature reactors (HTR) is very different in design: A fuel pebble consists of up to 10 000 small fuel kernels with diameters of about 500 µm, coated with pyrocarbon and silicon carbide (SiC), which are embedded in a moulded graphite sphere with a diameter of ≈60 mm (**Figure 2**). Furthermore, research reactors and materials test reactors mainly use aluminum-clad intermetallic fuels (e.g., UAl_x–Al and U_3Si_2–Al).

Due to neutron irradiation during reactor operation, the fuel material undergoes dramatic changes in its chemical composition and microstructure. More than one hundred short and long-lived radionuclides are formed due to fission and neutron capture reactions. Such SNF is a very complex and heterogeneous material in which solid solution phenomena play an important role.[4,32]

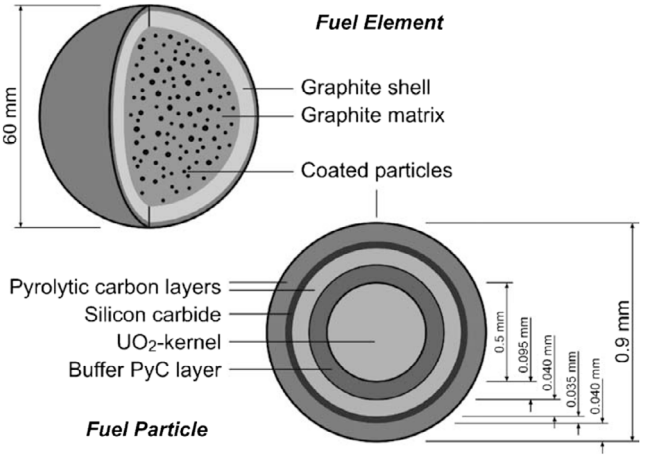

Figure 2. Design of an HTR fuel element and of a tristructural isotropic-coated fuel particle (modified after a previous study[31]). Reproduced with permission.[31] Copyright 2006, Elsevier.

Its radioactivity has increased by nine orders of magnitude (10^{19} Bq metric ton^{-1} of heavy metal) in comparison to unirradiated fuel. For example, the dose rate measured 1 m from the fuel assembly of a spent commercial light water reactor (LWR) fuel is 10^6 mSv h^{-1} (for comparison, the natural background dose is of the order of 2 mSv year^{-1} in Europe). A person exposed to this level of radioactivity would receive a lethal dose in less than a minute; hence, SNF must be handled remotely in a hot cell facility (**Figure 3**).[4,33] However, radioactivity (in Bq g^{-1}) and dose rate (in Sv h^{-1}) from SNF drop quickly and after 300–500 years, most beta and gamma emitters have decayed and alpha radiation will dominate the radiation field for several 100 000 years.

The temperature distribution in conventional UO_2/MOX fuel pellets during irradiation is not homogeneous, but a steep temperature gradient (several hundred degrees) between the hot center (up to 2000 °C) of the pellet (diameter: 10 mm) and the outer edge of the pellet (rim) exists. This gradient is mainly responsible for the radial heterogeneous segregation and distribution of the radionuclides. Due to mechanical stresses, further irradiation effects such as fuel swelling, pellet cracking, and pellet-cladding interaction are observed.

After unloading from the reactor after some years of operation, the SNF still contains 95 wt% of uranium oxide and about 5 wt% fission products as well as transuranium elements,[33] which can be classified into four groups:[34] 1) volatile and gaseous fission products (Kr, Xe, I) which can be found along grain boundaries, within intra and intergranular gas bubbles and in the gap between the fuel and cladding;[35] 2) fission products forming metallic precipitates (solid solutions) immiscible with the UO_2 matrix (Mo, Tc, Ru, Rh, Pd, Ag, Cd), so-called epsilon particles; 3) fission products forming complex solid solution oxide precipitates (Rb, Cs, Ba, Zr, Nb, Mo, Te); and 4) fission products (Sr, Zr, Nb, lanthanides) and actinides (Pu, Am, Cm) that are retained in the fuel matrix, forming solid solutions with UO_2. The morphological, macro-, and microstructural changes and the amount of fission products and activation products (produced by neutron capture) in SNF are highly dependent on the burn-up of the fuel.[36,37]

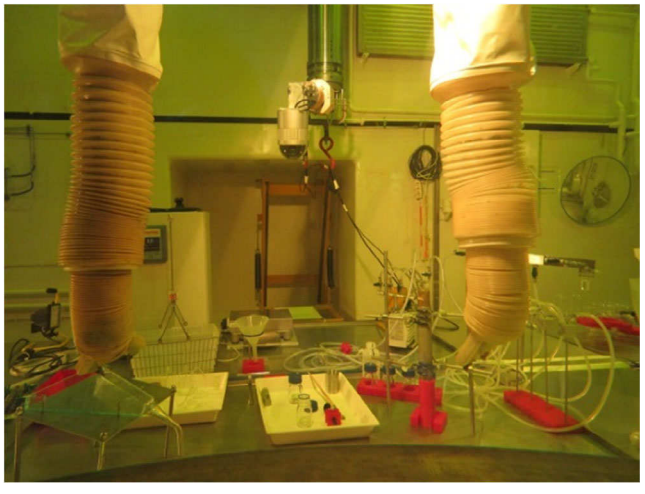

Figure 3. Static leaching experiment installed in a hot cell at Forschungszentrum Jülich.

Since (ground) water is considered as the principal pathway by which radionuclides could be transported from the waste material into the environment, the interaction of SNF with aqueous solution has been studied extensively (e.g., within collaborative European projects such as SFS, Micado, or First Nuclides) and a comprehensive view on corrosion phenomena of UO_2-based SNF has been developed in recent years.[4,33,36,38–40] The radionuclide release from SNF due to aqueous corrosion can be described by two components: 1) the fast (instant) release of radionuclides located in the rim and gap region and on grain boundaries (incl. ^{36}Cl, ^{79}Se, ^{129}I, ^{135}Cs), immediately after the fuel comes into contact with groundwater, and 2) the release of radionuclides due to the dissolution of the UO_2 matrix, which is driven by radiolysis due to alpha radiation in aqueous solution, thus forming locally oxidizing species (e.g., H_2O_2).[41–43]

In the following, the focus will be on recent corrosion studies performed at Forschungszentrum Jülich, related to less frequently investigated SNF materials, namely, HTR fuel, research reactor fuel, and MOX fuel.

3.1.1. HTR Fuel

Corrosion studies showed that the HTR fuel elements represent a very stable waste matrix as long as the integrity of the SiC coatings of the kernels is not impaired.[31,44,45] The instant release fraction from high burn-up (≈100 GWd t_{HM}^{-1}) HTR kernels (without SiC coating) is different compared to 60 GWd t_{HM}^{-1} LWR fuel and affected by the uniquely low oxygen potential within HTR fuel kernels.[46] Microscopic and microanalytical studies of irradiated HTR fuel kernels showed that, compared to LWR SNF, in this material the solid solutions in the metallic epsilon particles are enriched in Mo and contain unexpectedly high Zr concentrations.[46]

3.1.2. Research Reactor Fuel

Corrosion experiments of nonirradiated and irradiated research reactor fuel elements (UAl_x–Al and U_3Si_2–Al) in salt brines, clay waters, and granite waters revealed complete dissolution of these fuel types within a time frame of a few years.[47–51] The measured corrosion rates are up to four orders of magnitude larger than matrix corrosion rates of UO_2-based LWR fuels under similar conditions, with the highest corrosion rates in $MgCl_2$-rich brines and lower rates (about a factor 3) in clay and granite waters.

3.1.3. MOX Fuel

Dissolution experiments with irradiated MOX fuels (burn-up between 25.8 and 47.9 GWd t_{HM}^{-1}) were recently started in collaboration with Studiecentrum voor Kernenergie–Centre d'Etude de l'Energie Nucléaire (Mol, Belgium).[52] The leaching experiments are performed at ambient temperature in autoclaves pressurized at 40 bars with a mixture of 4 vol% H_2/Ar that are being operated in a hot cell facility. Both leachate solutions and the gas phase in the autoclaves are sampled, and the release behavior of more than 30 relevant radionuclides (including fission gases, actinides, and long-lived fission products) are determined by various analytical techniques. The aim is to study the SNF behavior

under deep geological repository conditions, addressing instant release and long-term matrix corrosion of irradiated MOX fuel in synthetic clay pore solution and cementitious pore waters.

Due to the chemical and structural complexities of SNF and its high radiation field, studies on "real" SNF samples cannot unravel all of the various mechanisms and processes contributing to the long-term matrix corrosion of SNF. Therefore, complementary studies are performed on simplified UO_2-based model systems in a tiered bottom-up approach. This approach has been successfully adopted in the European collaborative project DisCo.[53] Single-effect studies render to unravel and quantify the contributions of distinct reaction mechanisms at molecular scales to the overall long-term SNF matrix corrosion. Specifically, the following aspects are currently investigated to address open issues related to SNF corrosion: 1) lanthanide fission products in solid solution with the UO_2 matrix are known to affect SNF corrosion rates, but the detailed mechanism remains unclear so far;[54–57] 2) Cr doping is used during fuel production to increase its performance during reactor operation,[58,59] but the impact of the Cr dopants, partly in solid solution with UO_2, on SNF corrosion is not known to date;[60–62] 3) the threshold value for alpha-radiolysis-driven UO_2 matrix corrosion; 4) the potential catalytic contribution of the epsilon particles, including their chemical composition (solid solution), on the SNF redox reactivity; and 5) the effect of the nature of the SNF matrix microstructure on SNF alteration mechanisms.

The outcome of these SNF corrosion studies outlined earlier contributed to the scientific basis for the derivation of respective source terms in the preliminary safety assessment for a geological repository at the German Gorleben site ("vorläufige Sicherheitsanalyse Gorleben", vSG).[63]

3.2. Retention of Radium within the Repository System

Secondary phases are considered as relevant materials in nuclear waste management due to their potential for radionuclide retention.[64,65] In some safety cases they are considered as components in the multibarrier system. A prerequisite for the applicability of this SS–AS system is a complete set of thermodynamic data and their experimental confirmation. Here, an interdisciplinary approach was applied focusing on the material properties of the solid. A combination of batch-type laboratory experiments was complemented by state-of-the-art analytical techniques, atomistic simulations, and thermodynamic modeling approaches.

Depending on the environmental conditions, the aqueous concentration of Ra in a high-level nuclear waste repository can be controlled by sulfate minerals. The first aim of the experimental approach was the validation of the concept that pure barite ($BaSO_4$) in contact with a Ra-containing solution would evolve to a (Ba, Ra)SO_4 solid solution via a recrystallization mechanism. Batch recrystallization experiments and detailed analyses of the solid and aqueous phases were conducted at defined times. Even though recrystallization is usually considered to be a rather slow process, already after 443 days the uptake of Ra into the bulk of barite was confirmed via ToF-SIMS (**Figure 4**), indicating close-to-equilibrium conditions.[66] In fact, by combining known

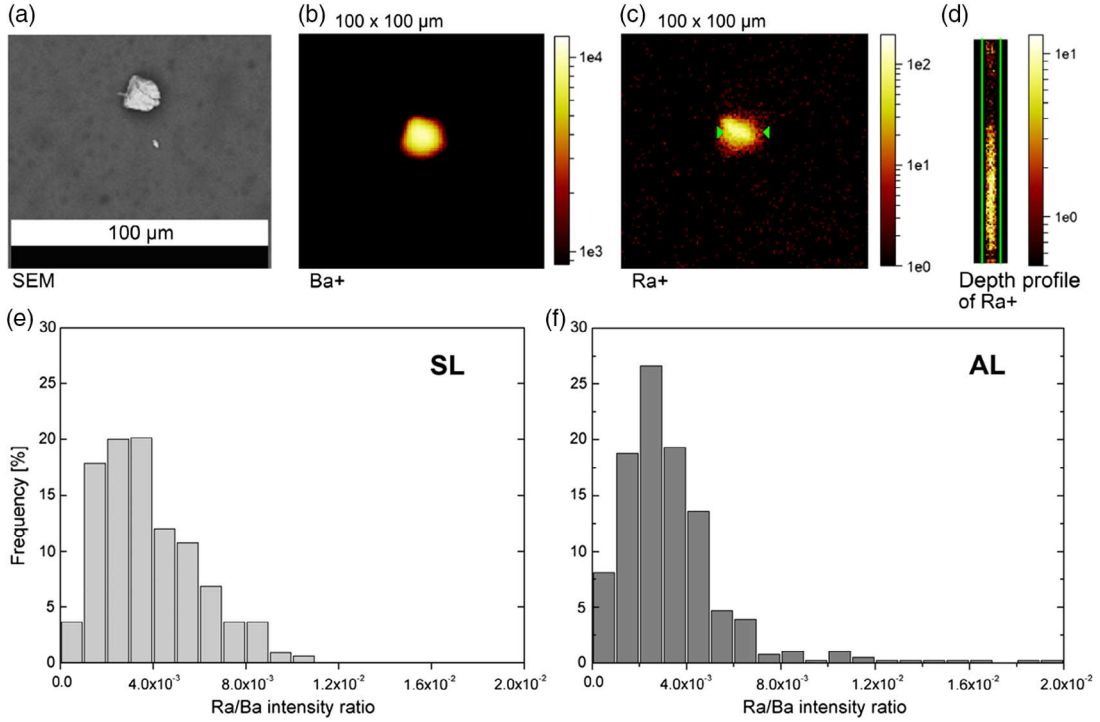

Figure 4. a) SEM image of barite particle before ToF-SIMS analysis, b) integrated intensity of the Ba signal, c) integrated intensity of the Ra signal, d) depth profile of the integrated Ra signal. e) Histogram of the Ra/Ba ToF-SIMS intensity ratio obtained from 660 integrated measurement points of SL (Sachtleben) 0.5 g L^{-1}. f) Histogram of the Ra/Ba ToF-SIMS intensity ratio obtained from 400 integrated measurement points of AL (Aldrich) 0.5 g L^{-1}. Reproduced with permission.[65,66] Copyright 2014, American Chemical Society, copyright 2016, Elsevier.

solubility products of the end members with the corresponding Ra/Ba ratios obtained from ToF-SIMS the experimental regular solution interaction parameter was estimated.[66] The latter was comparable to the interaction parameter derived ab initio.[8,67] A deeper understanding of the relevant properties of barite that enable the surprisingly high Ra uptake was obtained by using APT and HRTEM, combined with high-resolution microchemical analysis (energy-dispersive X-ray spectroscopy, EDX).[68,69] The characterization of the pristine synthetic barite showed that it contained significant amounts of pores in the micrometer to nanometer scale (**Figure 5**a,b). Macropores connecting the surface with the inside of the particles were observed together with nanoscale pores; the latter were identified as strata of fluid inclusions (Figure 5c). During the recrystallization of barite in the presence of Ra, these pores provided fast pathways for Ra into the solid due to dissolution–reprecipitation processes. TEM–EDX investigations revealed an inhomogeneous distribution of Ra among (Ba, Ra)SO_4 particles at intermediate stages of the recrystallization and an enrichment of Ra around micrometer-scaled pores (Figure 5d,e). Detailed analyses of (Ba, Ra)SO_4 with FIB cross-sectioning taken at different recrystallization times indicated a dynamic restructuring of these fluid inclusions during the uptake of Ra, destroying their initial stratified arrangement and leading to a more homogeneous solid solution. In some kind of a ripening process, many nanoscaled pores disappeared in favor of a smaller number of macropores. In summary, these results justified the assumption that in relatively short time scales a full recrystallization of barite to a (Ba, Ra)SO_4 solid solution is possible, favored by the internal porous structure of barite.

The largest uncertainty within the available thermodynamic dataset for (Ba, Ra)$SO_4 + H_2O$ was due to the poorly known thermodynamic activity of the $RaSO_4$ end member within the (Ba, Ra)SO_4 solid solution. The specific approach developed here was to combine atomistic DFT-based calculations with thermodynamic modeling of SS–AS equilibria, using the software package GEM-Selektor.[70] The regular model interaction parameter W was computed ab initio with the single defect method from the enthalpy increase of a $2 \times 2 \times 2$ supercell of $BaSO_4$ (**Figure 6**) due to the insertion of a single substitutional defect of Ra. Details of these calculations are given in Vinograd et al.[8,14]

The W_{BaRa} parameter was determined to be $2.5 \pm 1.0\,kJ\,mol^{-1}$, indicating a slightly nonideal solid solution. Further effort was undertaken to assess the asymmetry of the mixing properties within the (Ba, Ra)SO_4 solid solution and to estimate effects of chemical ordering,[14] the heat capacity of $RaSO_4$, and the effects of temperature on the aqueous equilibria of the SS–AS system (Ba, Ra)$SO_4 + H_2O$.[10] These predictions indicated a relative increase in the solubility of the $RaSO_4$ end member with increasing temperature, causing a slight increase in the aqueous Ra concentration in the presence of a given amount of $BaSO_4$.

In summary, our results provided a detailed justification of the concept that in the SS–AS (Ra, Ba)$SO_4 + H_2O$ system the aqueous

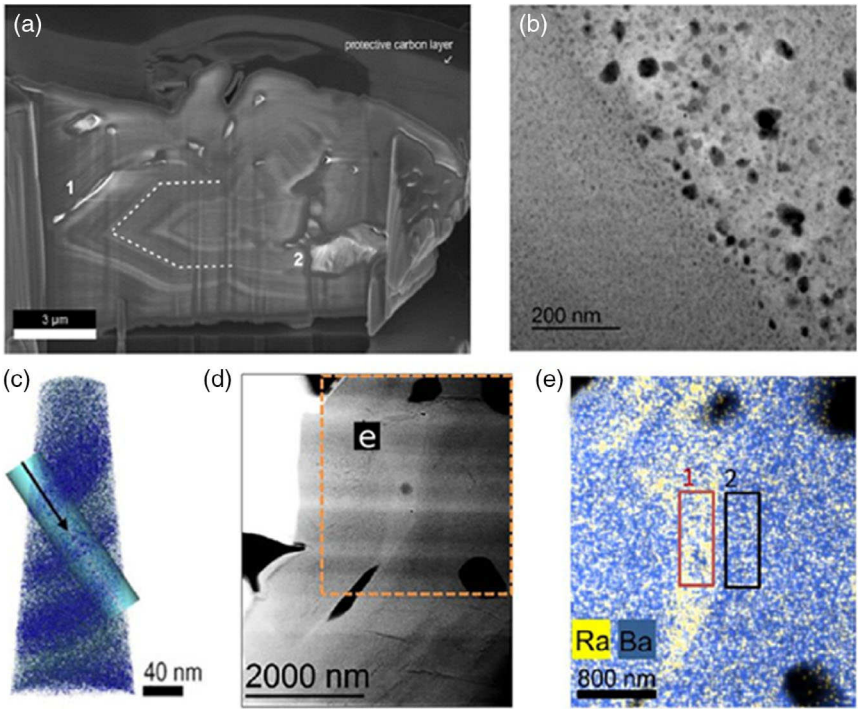

Figure 5. a) Cross-section of a synthetic barite particle containing a layered structure, (1) elongated pores and (2) larger, randomly oriented pores. b) High-angle annular dark-field–scanning transmission electron microscope (HAADF-STEM) image of pristine barite c) 3D elemental composition reconstructions of an APT measurement of a synthetic barite of the same type, green: Ba, blue: H_2O; d,e) Ra distribution inside the barite at intermediate stage of the recrystallization. HAADF-STEM image and corresponding STEM-EDX mapping of the indicated area. Reproduced with permission.[68,69] Copyright 2016, 2017, Elsevier.

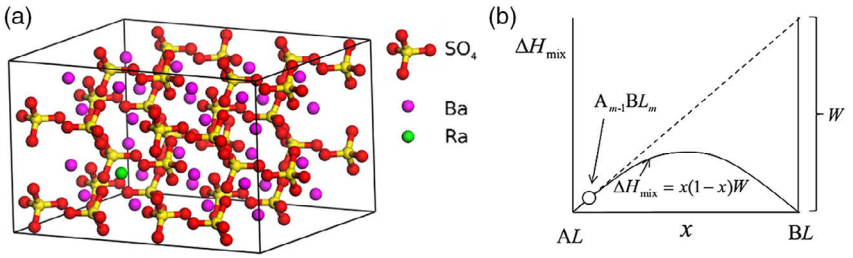

Figure 6. a) A $2 \times 2 \times 2$ supercell of $BaSO_4$ with one substitutional defect; b) relationship between the enthalpy of mixing in the regular model and the parameter *W*: *W* is equal to the slope to the enthalpy of mixing function in the limit of $x = 0$. Adapted from Vinograd et al.[8] Reproduced with permission.[8] Copyright 2013, Elsevier.

solubility of Ra would be orders of magnitude lower than in the system of $RaSO_4 + H_2O$. Our studies allowed closing knowledge gaps in thermodynamic properties of the relevant phases and proved the applicability of recrystallization as the main mechanism of solid-solution formation to be considered in safety assessments for nuclear waste repositories. Particularly, by comparing experimental data with results of atomistic simulations and thermodynamic modeling it was shown that the thermodynamic equilibrium can be closely achieved in the SS–AS system (Ba, Ra)$SO_4 + H_2O$ within the time interval of 2–3 years. Ra-sulfate SS–AS systems are already considered in safety assessments for the Swiss, the Swedish, and the Finnish safety cases for deep geological HLW repositories.[71–74] The research was recently extended to the ternary (Ba, Sr, Ra)$SO_4 + H_2O$ system where the thermodynamic models and approaches described previously were successfully applied.[14,75,76]

3.3. Pyrochlore-Type Ceramic Waste Forms

For many nuclear waste streams some form of treatment and conditioning is required prior to disposal to render them into solid waste forms. A number of immobilization techniques have been established throughout the last decades, e.g., cementation of low- and intermediate-level wastes[77–79] or vitrification of HLW streams generated in the course of reprocessing of SNF.[80–83] Moreover, a variety of single-phase and poly-phase ceramic matrices (based, e.g., on oxides such as pyrochlore and zirconolite, silicates such as zircon, or phosphates such as monazite) have been explored as potential alternative waste matrices for specific waste streams such as separated plutonium from civilian or military sources unsuitable for further use, minor actinides (Am, Cm, Np), or long-lived fission products.[84–97] In these crystalline ceramics, selected in particular for their high chemical durability and radiation stability, radionuclides can be incorporated into the lattice structure of the host phase occupying specific atomic positions, which allows for high loadings of specific radionuclides.

As shown in **Figure 7**, pyrochlore has the general formula $A_2B_2O_7$ and can be described as a derivative of the (cubic) fluorite structure. The pyrochlore structure offers a great deal of chemical flexibility, allowing for the incorporation of trivalent lanthanides as well as of tri- and tetravalent actinides;[91] the latter may be incorporated on both the A- and B-sites. The enhanced radiation damage resistance of specific pyrochlore compounds (e.g., $Gd_2Zr_2O_7$) is realized under irradiation by the formation of a disordered solid phase called defect fluorite (Figure 7).[88]

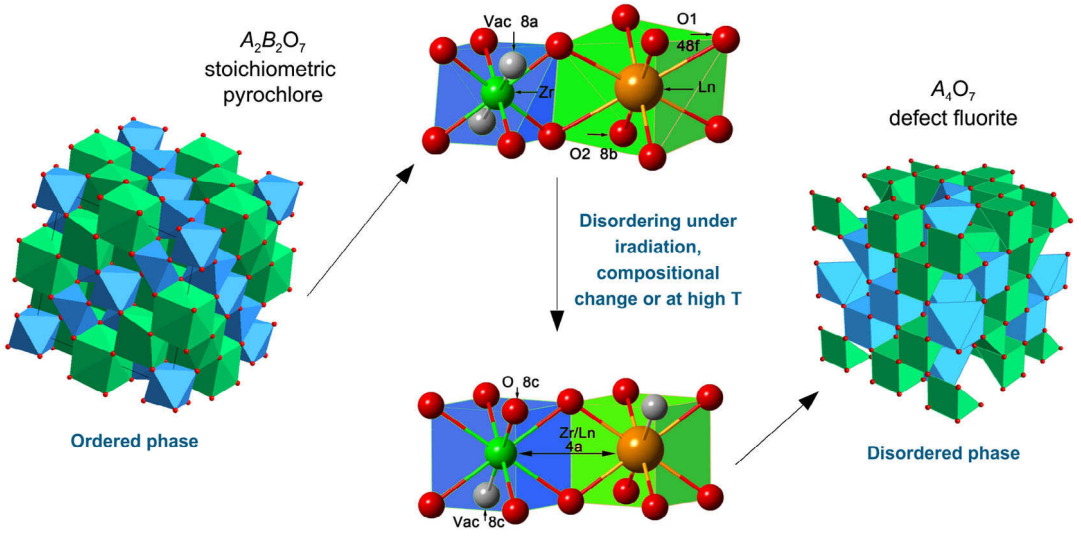

Figure 7. Schematic representation of the structure of pyrochlore (zirconate: $Ln_2Zr_2O_7$) and its disordered phase.

For instance, experiments on self-irradiated $Gd_2(Ti,Zr)_2O_7$ materials containing 10 wt% ^{239}Pu show that so-irradiated $Gd_2Ti_2O_7$ will be amorphized in ≈1000 years, while in $Gd_2Zr_2O_7$ amorphization will not occur at all.[88] However, the underlying mechanisms that cause this phenomenon are still poorly understood. For instance, it has not been conclusively demonstrated which atomic scale process is the driver behind the order–disorder transition, how the transition proceeds under temperature and pressure, how fast the radiation damage–resistant compounds dissolve, and most importantly, how actinides such as Pu are incorporated into their matrix.

Fundamental properties of pyrochlore materials are investigated to understand their overall performance as a nuclear waste form. Research using a large variety of experimental techniques and advanced first-principles-based simulation techniques has been performed. Most importantly, a synergy of experiment, simulation, and theory has been applied to obtain the best possible characterization of the processes of interest. The new knowledge gains and predictions made were validated on many occasions by follow-up independent experimental studies.

One of the key topics in characterization of a crystalline nuclear waste form is to understand the structural incorporation of radionuclides (e.g., actinides) into its structure. In that aspect, the investigation of local structures in pyrochlore-type materials, including probes doped with f-elements, has been performed. Time resolved laser-induced fluorescence spectroscopy has been used to probe the local environment of Eu^{3+} and Cm^{3+} in $La_2Zr_2O_7$ with pyrochlore and defect fluorite structure.[98] It resulted in the detection of well-defined eightfold environments of dopant cations in pyrochlore and low-symmetry doping positions in case of defect fluorite, as expected due to the disordered nature of the latter material. All the dopants were completely incorporated into the crystalline lattice. In addition, the nuclear inelastic scattering has been used to investigate the lattice dynamics in $(Eu, Nd)_2Zr_2O_7$.[99] These measurements indicate strong broadening of phonon modes resulting from the loss of locally symmetric coordination of Zr and due to the softening of the pyrochlore framework upon the Eu incorporation. Moreover, a Mössbauer spectroscopy study of the $Eu_{1-x}Nd_xZr_2O_7$ system revealed significant changes in the isomer shift and quadruple splitting, indicating distinct differences in the local structure of pyrochlore and defect fluorite.[100]

Although experiments with lanthanides as surrogates for actinides provide valuable clues about the structural incorporation of actinides and the performance of the formed solid solutions, only studies of pyrochlore-type solid solutions with actinides could provide a complete understanding of the performance of pyrochlore as a waste form. This is in part because actinides show a more complex redox chemistry than lanthanides, with Pu exhibiting a variety of oxidation states (e.g., Pu(III) or Pu(IV)). We thus performed joint experimental and simulation investigations of Pu-doped $Nd_2Zr_2O_7$ pyrochlore.[101] The analyzed XANES data suggested a tetravalent state of Pu, but EXAFS data indicated a coordination environment, resembling doping on the crystallographic position of Nd. This finding was supported by the ab initio calculation of Pu solution energies in pyrochlore.

In the investigation of the local structural atomic arrangements in pyrochlore-based waste forms, an important question is on the extent of preservation of atomic ordering (short-range order) in the disordered defect fluorite phase. By neutron total scattering, a significant local short-range ordering of weberite type in defect fluorite materials has been detected.[102] These results have been supported by joint experimental [X-ray diffractometry (XRD), thermochemistry] and atomistic modeling studies, which characterized the thermochemistry, the thermodynamics, and the evolution of structural parameters of the $Nd_xZr_{1-x}O_{2-0.5x}$ system that undergoes composition induced order–disorder phase transition.[30] As shown in **Figure 8**, the measured low entropy of disordering of 16 J mol^{-1} K^{-1} fits into the picture of significant short-range ordering of weberite type in defect fluorite phases as proposed by Shamblin et al.[102]

The atomistic modeling is an integral part of the research approach presented here and, as already shown, it has been frequently used to support the experimental effort for understanding the experimental data. However, a pure simulation driven research that aims at understanding the performance of pyrochlore as a nuclear waste form on the atomic scale has also been applied. The adequate and accurate computational methodology (see Section 2) substantially improved the DFT prediction of the temperature of order–disorder transitions and allowed for derivation of accurate maps of cation antisite and anion Frenkel pair defect formation energies[27,103] (**Figure 9**), which were recently shown to be the best match to the experimental values.[104] As shown in Figure 9, the obtained maps reveal a clear correlation between the oxygen Frenkel pair defect formation energies and the stability field of pyrochlore. Li et al.[27] showed that the compounds that form defect fluorite have small or negative Frenkel pair defect formation energy. In addition, the activation barriers for oxygen diffusion computed by Li and Kowalski[105] are consistent with the experimentally measured values and trends. For instance, they explained the maximum ionic conductivity observed in the zirconium–pyrochlore series of Eu by

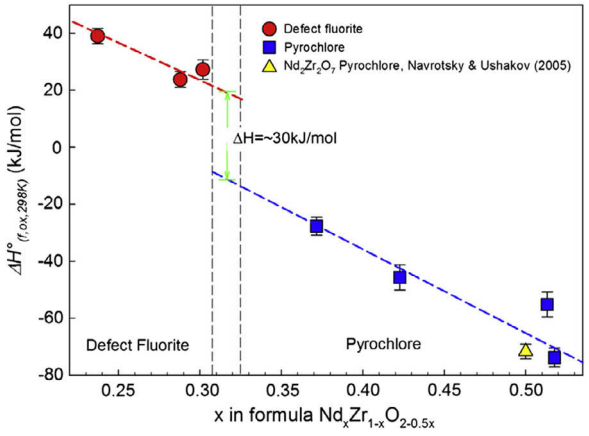

Figure 8. The calorimetric measurements of enthalpy of formation from oxides in $Nd_xZr_{1-x}O_{2-0.5x}$ system. The indicated enthalpy of the pyrochlore to defect fluorite transition of $\Delta H = 30$ kJ mol^{-1} corresponds to the transition entropy of 16 J mol^{-1} K^{-1}.[30] Reproduced with permission.[30] Copyright 2017, Elsevier.

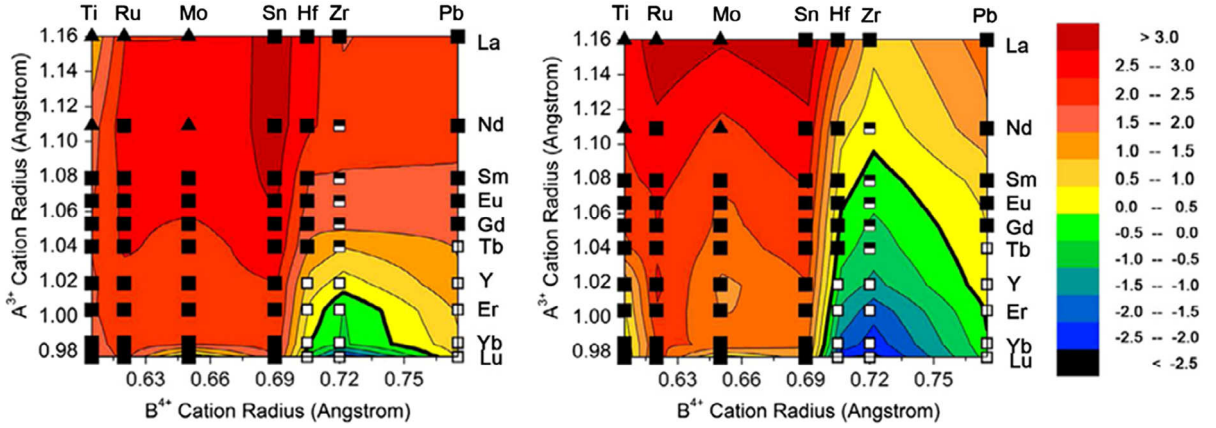

Figure 9. The contour maps of the cation antiside (left) and anion Frenkel pair (rights) defect formation energies for series of pyrochlore compositions. Symbols represent the most stable phase: pyrochlore (filled square), pyrochlore that transforms to disordered fluorite at temperature (half-filled squares), defect fluorite (empty squares), and noncubic phases (filled triangles). Reproduced with permission.[27] Copyright 2015, Elsevier.

formation of a split vacancy state for heavier lanthanides. These computational studies demonstrated that disordering enhances oxygen diffusion and that the flexibility of the oxygen sublattice is a driver for the disordering transition and the related radiation damage resistance of pyrochlore.

Another important aspect of the research on solid nuclear waste forms is the understanding of their behavior when in contact with aqueous solutions. A series of studies aiming at the understanding of the dissolution process have been performed. The kinetics of dissolution has been investigated at both the macroscopic and microscopic level, using advanced techniques, such as vertical scanning interferometry (VSI), scanning electron microscopy (SEM), environmental scanning electron microscopy, atomic force microscopy, X-ray reflectometry, XRD, mössbauer spectroscopy. Wet chemical analysis and detailed SEM studies indicate preferential leaching at grain boundaries, showing no significant influence of the structure type (pyrochlore or defect fluorite) on the dissolution rate.[106,107] VSI allowed for the evaluation of different contributions to the total dissolution rate of $Nd_2Zr_2O_7$, including the single grain dissolution, the dissolution at grain boundaries, at triple point junctions, and the erosion of pulled-out partly dissolved pyrochlore grains (**Figure 10**).[108] The identification of individual contributing processes provides also a new way of analysis of reaction rates in polycrystalline materials. Highly heterogeneous dissolution was also observed by Szenknect et al. (**Figure 11**).[109] These studies suggest that the stability of pyrochlore materials against chemical corrosion is enhanced by an increase in the average grain size.

The combination of experimental and atomistic modeling studies discussed here yields a more detailed insight into the mechanism of the structural immobilization of actinides in pyrochlore-type solid solutions, the thermodynamic parameters of such waste forms, and the structural disordering causing the enhanced radiation damage resistance of selected pyrochlore compounds. The obtained results contribute to the understanding of the long-term behavior of pyrochlore-type ceramics as a nuclear waste form.

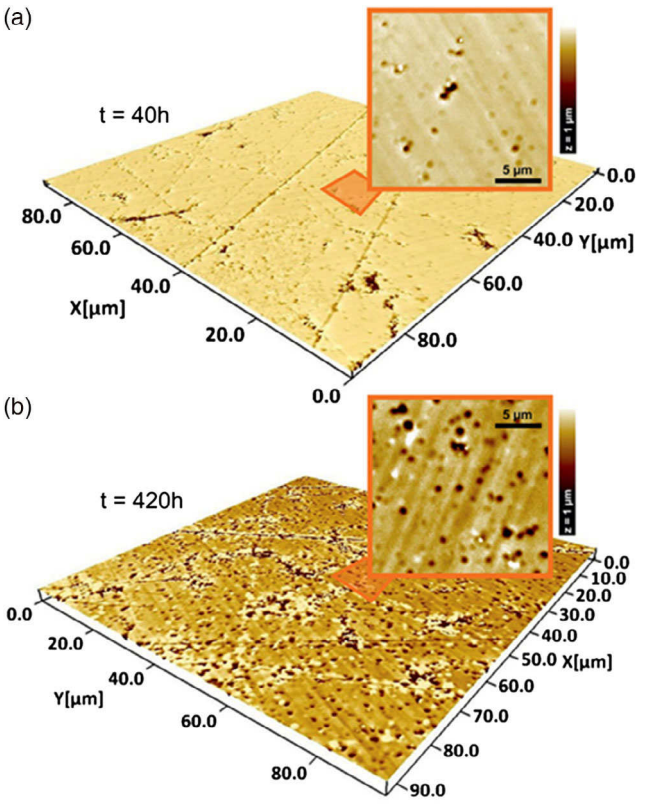

Figure 10. Evolution of pyrochlore sample surface topography after dissolution during a) 40 h and b) 420 h. Reproduced with permission.[108] Copyright 2015, American Chemical Society.

4. Conclusions

The safe management of radioactive wastes and in particular their final disposal in a deep geological repository requires an in-depth understanding of the long-term behavior of the materials involved, including the radionuclides present in the

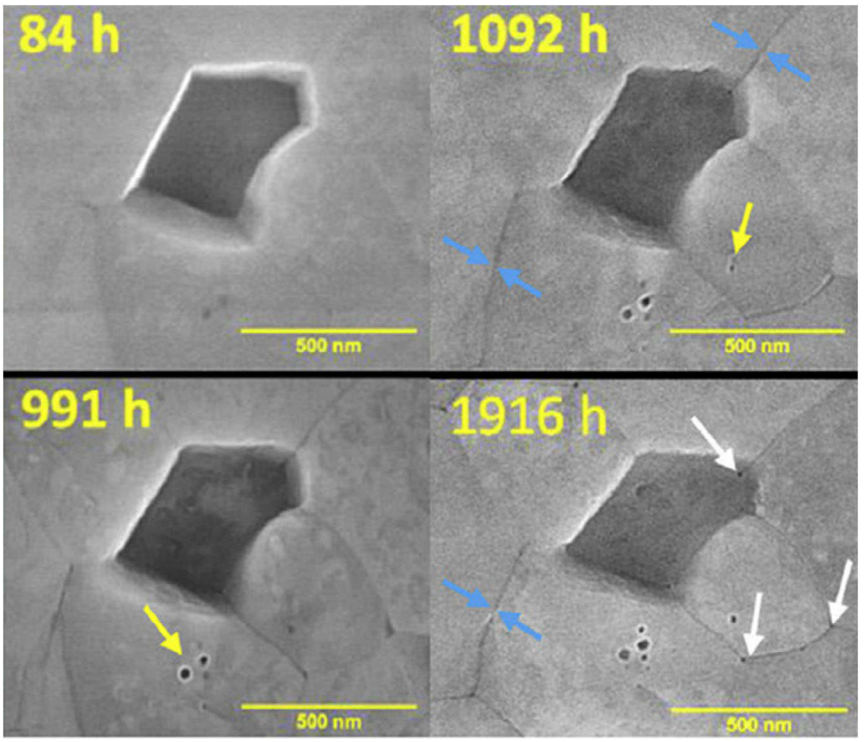

Figure 11. SEM images of the selected region of $Nd_2Zr_2O_7$ sample surface depending on dissolution time (h). Blue, yellow, and white arrows indicate the dissolution of the grain boundaries, the digging of the corrosion pits, and the opening of the triple points, respectively. Reproduced with permission.[109] Copyright 2017, Elsevier.

nuclear waste forms. Therefore, materials research is an essential element in the provision of the knowledge base for the assessment of the (long-term) evolution of the repository system, contributing thus to the scientific basis of the safety case. Various countries have advanced nuclear waste disposal programs for high-level radioactive wastes; the respective safety cases demonstrate the safety of the (planned) waste repositories. The respective safety assessments are based particularly on a good phenomenological understanding of the processes affecting the materials in the multibarrier system and the repository evolution over time, and a number of conservative assumptions. However, to further substantiate the long-term safety of the repositories, a refined mechanistic process understanding, based on state-of-the-art science, is beneficial to improve the confidence in predictions on repository system evolution over the required time scales of up to 1 million years. By integrating innovative experimental approaches and advanced simulation methods (at various length and time scales), a number of open issues with respect to the behavior of (waste) materials in the repository environment have been successfully addressed at Forschungszentrum Jülich in recent years. Remaining topics to be addressed within this context comprise, inter alia, coupled processes at materials interfaces within the multibarrier system of a repository, specific reaction mechanisms affecting SNF corrosion such as the H_2-effect, and the performance of innovative waste forms for special nuclear waste streams under repository conditions.

Conflict of Interest

The authors declare no conflict of interest.

Keywords

materials science aspects, nuclear wastes, solid solutions

Received: November 19, 2019
Revised: January 27, 2020
Published online: February 28, 2020

[1] Council of the European Union (CEC), *Council directive 011/70/EURATOM of 19 July 2011 Establishing a Community Framework for the Responsible and Safe Management of Spent Fuel and Radioactive Waste*, CEC, Brussels, Belgium **2011**.
[2] International Atomic Energy Agency (IAEA), *Scientific and Technical Basis for the Geological Disposal of Radioactive Wastes, Technical Reports Series 413*, IAEA, Vienna, Austria **2004**.
[3] D. G. Bennett, R. J. Gens, *J. Nucl. Mater.* **2008**, *379*, 1.
[4] P. Carbol, D. H. Wegen, T. Wiss, P. Fors, *Compr. Nucl. Mater.* **2012**, *5*, 389.
[5] F. King, *Compr. Nucl. Mater.* **2012**, *5*, 422.
[6] L. Bourgeois, P. Dehaudt, C. Lemaignan, A. Hammou, *J. Nucl. Mater.* **2001**, *297*, 313.
[7] M. Prieto, *Rev. Mineral. Geochem.* **2009**, *70*, 47.
[8] V. L. Vinograd, F. Brandt, K. Rozov, M. Klinkenberg, K. Refson, B. Winkler, D. Bosbach, *Geochim. Cosmochim. Acta* **2013**, *122*, 398.

[9] F. Grandia, J. Merino, J. Bruno, *Assessment of the Radium–Barium Co-Precipitation and Its Potential Influence on the Solubility of Ra in the Near-Field, Technical Report TR-08-07*, Svensk Kärnbränslehantering AB, Stockholm, Sweden **2008**.
[10] V. L. Vinograd, D. A. Kulik, F. Brandt, M. Klinkenberg, J. Weber, B. Winkler, D. Bosbach, *Appl. Geochem.* **2018**, *93*, 190.
[11] M. Prieto, A. Fernandez-Gonzalez, A. Putnis, L. Fernandez-Diaz, *Geochim. Cosmochim. Acta* **1997**, *61*, 3383.
[12] M. H. F. Sluiter, Y. Kawazoe. *Europhys. Lett.* **2002**, *57*, 526.
[13] Y. Li, P. M. Kowalski, A. Blanca-Romero, V. Vinograd, D. Bosbach, *J. Solid State Chem.* **2014**, *220*, 137.
[14] V. L. Vinograd, D. A. Kulik, F. Brandt, M. Klinkenberg, J. Weber, B. Winkler, D. Bosbach, *Appl. Geochem.* **2018**, *89*, 59.
[15] X.-D. Wen, R. L. Martin, T. M. Henderson, G. E. Scuseria, *Chem. Rev.* **2013**, *113*, 1063.
[16] P. M. Kowalski, G. Beridze, Y. Ji, Y. Li, *MRS Adv.* **2017**, *2*, 491.
[17] A. Blanca-Romero, P. M. Kowalski, G. Beridze, H. Schlenz, D. Bosbach, *J. Comput. Chem.* **2014**, *35*, 1339.
[18] P. M. Kowalski, G. Beridze, Y. Li, Y. Ji, C. Friedrich, E. Şaşıoğlu, S. Blügel, *Ceram. Trans.* **2016**, *258*, 207.
[19] G. Beridze, P. M. Kowalski, *J. Phys. Chem. A* **2014**, *118*, 11797.
[20] G. Beridze, A. Birnie, S. Koniski, Y. Ji, P. M. Kowalski, *Prog. Nucl. Energy* **2016**, *92*, 142.
[21] S. Biswas, S. J. Edwards, Z. Wang, H. Si, L. L. Vintró, B. Twamley, P. M. Kowalski, R. J. Baker, *Dalton Trans.* **2019**, *48*, 13057.
[22] M. I. Lelet, M. L. Borodulina, P. M. Kowalski, E. V. Suleimanov, C. A. Geiger, E. V. Alekseev, *J. Chem. Thermodyn.* **2019**, *139*, 105873.
[23] B. Xiao, T. M. Gesing, L. Robben, A. Blanca-Romero, P. M. Kowalski, Y. Li, P. Kegler, V. Klepov, D. Bosbach, E. V. Alekseev, *Chemistry Eur. J.* **2016**, *22*, 946.
[24] G. L. Murphy, C. H. Wang, G. Beridze, Z. Zhang, J. A. Kimpton, M. Avdeev, P. M. Kowalski, B. J. Kennedy, *Inorg. Chem.* **2018**, *57*, 5948.
[25] K. Kvashnina, P. M. Kowalski, S. Butorin, G. Leinders, J. Pakarinen, R. Bes, H. Li, M. Verwerft, *Chem. Comm.* **2018**, *54*, 9757.
[26] G. Murphy, C. H. Wang, Z. Zhang, P. M. Kowalski, G. Beridze, M. Avdeev, O. Muransky, H. Brand, Q. Gu, B. Kennedy, *Inorg. Chem.* **2019**, *58*, 6143.
[27] Y. Li, P. M. Kowalski, G. Beridze, A. R. Birnie, S. Finkeldei, D. Bosbach, *Scr. Mater.* **2015**, *107*, 18.
[28] Y. Ji, P. M. Kowalski, S. Neumeier, G. Deissmann, P. K. Kulriya, J. D. Gale, *Nucl. Instrum. Methods Phys. Res. B* **2017**, *393*, 54.
[29] P. M. Kowalski, Y. Li, *J. Eur. Ceram. Soc.* **2016**, *36*, 2093.
[30] S. Finkeldei, P. Kegler, P. M. Kowalski, C. Schreinemachers, F. Brandt, A. A. Bukaemskiy, V. L. Vinograd, G. Beridze, A. Shelyug, A. Navrotsky, D. Bosbach, *Acta Mater.* **2017**, *25*, 166.
[31] J. Fachinger, M. den Exter, B. Grambow, S. Holgersson, C. Landesman, M. Titov, T. Podruhzina, *Nucl. Eng. Des.* **2006**, *236*, 543.
[32] H. Kleykamp, J. O. Paschoal, R. Pejsa, F. Thummler, *J. Nucl. Mater.* **1985**, *130*, 426.
[33] J. Bruno, R. C. Ewing, *Elements* **2006**, *2*, 343.
[34] H. Kleykamp, *Nucl. Technol.* **1988**, *80*, 412.
[35] J. Rest, M. W. D. Cooper, J. Spino, J. A. Turnbull, P. Van Uffelen, C. T. Walker, *J. Nucl. Mater.* **2019**, *513*, 310.
[36] R. C. Ewing, *Nat. Mater.* **2015**, *14*, 252.
[37] V. V. Rondinella, T. Wiss, *Mater. Today* **2010**, *13*, 24.
[38] D. W. Shoesmith, *J. Nucl. Mater.* **2000**, *282*, 1.
[39] K. Spahiu, J. Devoy, D. Cui, M. Lundström, *Radiochim. Acta* **2004**, *92*, 597.
[40] T. Fanghänel, V. V. Rondinella, J.-P. Glatz, T. Wiss, D. H. Wegen, T. Gouder, P. Carbol, D. Serrano-Purroy, D. Papaioannou, *Inorg. Chem.* **2013**, *52*, 3491.
[41] L. Johnson, C. Ferry, C. Poinssot, P. J. Lovera, *J. Nucl. Mater.* **2005**, *346*, 56.
[42] C. Poinssot, C. Ferry, P. Lovera, C. Jegou, J. M. Gras, *J. Nucl. Mater.* **2005**, *346*, 66.
[43] K. Lemmens, E. Gonzalez-Robles, B. Kienzler, E. Curti, D. Serrano-Purroy, R. Sureda, A. Martínez-Torrents, O. Roth, E. Slonszki, T. Mennecart, I. Günther-Leopold, Z. Hozer, *J. Nucl. Mater.* **2017**, *484*, 307.
[44] J. Fachinger, H. Brücher, R. Duwe, *Technologies for Gas Cooled Reactor Decommissioning, Fuel Storage and Waste Disposal* (Ed: IAEA), International Atomic Energy Agency, Vienna, Austria **1997**.
[45] H. Rainer, J. Fachinger, *Radiochim. Acta* **1998**, *80*, 139.
[46] H. Curtius, G. Kaiser, N. Lieck, M. Güngör, M. Klinkenberg, D. Bosbach, *Radiochim. Acta* **2015**, *103*, 433.
[47] J. Fachinger, H. Curtius, *Applied Mineralogy in Research, Economy, Technology, Ecology and Culture* (Eds.: D. Rammlmair, J. Mederer, T. Oberthür, R. B. Heimann, H. Pentinghaus), A. A. Balkema, Rotterdam, The Netherlands **2000**.
[48] L. Mazeina, H. Curtius, J. Fachinger, R. Odoj, *J. Nucl. Mater.* **2003**, *321*, 1.
[49] H. Curtius, G. Kaiser, E. Müller, D. Bosbach, *J. Nucl. Mater.* **2011**, *416*, 211.
[50] M. Klinkenberg, A. Neumann, H. Curtius, G. Kaiser, D. Bosbach, *Radiochim. Acta* **2014**, *102*, 311.
[51] A. Neumann, M. Klinkenberg, H. Curtius, *Radiochim. Acta* **2017**, *105*, 85.
[52] G. Leinders, T. Mennecart, G. Cornelis, G. Verpoucke, G. Modolo, D. Bosbach, K. Lemmens, M. Verwerft, presented at Top Fuel 2019 Conf., Seattle, WA September **2019**.
[53] L. Zetterström-Evins, presented at EURADWASTE 2019, Pitesti, Romania June **2019**.
[54] C. Schreinemachers, A. A. Bukaemskiy, M. Klinkenberg, S. Neumeier, G. Modolo, D. Bosbach, *Prog. Nucl. Energy* **2014**, *72*, 17.
[55] S. Finkeldei, F. Brandt, G. Deissmann, A. Bukaemskiy, M. Lang, R. Ewing, D. Bosbach, presented at MRS Fall Meeting, Boston, MA, November **2016**.
[56] S. Finkeldei, A. Baena, R. Palomares, F. Brandt, G. Deissmann, A. Bukaemskiy, M. Lang, R. Ewing, D. Bosbach, presented at Goldschmidt, Paris August **2017**.
[57] S. Finkeldei, A. Baena, F. Brandt, G. Deissmann, M. Klinkenberg, R. Palomares, M. Lang, A. Maier, M. Jonsson, R. Ewing, D. Bosbach, presented at MRS Fall Meeting, Boston, MA, November **2017**.
[58] J. Arborelius, K. Backman, L. Hallstadius, M. Limbäck, J. Nilsson, B. Rebensdorff, G. Zhou, K. Kitano, R. Löfström, G. Rönnberg, *J. Nucl. Sci. Technol.* **2006**, *43*, 967.
[59] A. R. Massih, *Effects of Additives on Uranium Dioxide Fuel Behaviour, SSM Report*, Vol. *21*, Strålsäkerhetsmyndigheten SSM, Stockholm, Sweden **2014**.
[60] F. Brandt, P. Kegler, S. Lange, M. Klinkenberg, A. Bukaemskiy, G. Deissmann, S. Finkeldei, D. Bosbach, presented at MRS Fall Meeting, Boston, MA, November **2018**.
[61] P. Kegler, M. Klinkenberg, A. Bukaemskiy, G. Deissmann, D. Bosbach, E. V. Alekseev, R. Delville, C. Cachoir, T. Mennecart, K. Lemmens, M. Verwerft, presented at EURADWASTE, Pitesti, Romania June **2019**.
[62] P. Kegler, M. Klinkenberg, A. Bukaemskiy, F. Brandt, G. Deissmann, D. Bosbach, presented at Spent Fuel Workshop, Ghent, Belgium **2019**.
[63] B. Kienzler, M. Altmaier, C. Bube, V. Metz, *KIT Sci. Rep.* **2013**, *7365*, 1.
[64] J. Bruno, D. Bosbach, D. Kulik, A. Navrotsky, *Chemical Thermodynamics of Solid Solutions of Interest in Nuclear Waste Management: A State-of-the-Art Report*, OECD Nuclear Agency (NEA), Paris **2007**.

[65] M. Prieto, F. Heberling, R. M. Rodríguez-Galán, F. Brandt, *Prog. Cryst. Growth Charact. Mater.* **2016**, *62*, 29.
[66] M. Klinkenberg, F. Brandt, U. Breuer, D. Bosbach, *Environ. Sci. Technol.* **2014**, *48*, 6620.
[67] F. Brandt, E. Curti, M. Klinkenberg, K. Rozov, D. Bosbach, *Geochim. Cosmochim. Acta* **2015**, *155*, 1.
[68] J. Weber, J. Barthel, F. Brandt, M. Klinkenberg, U. Breuer, M. Kruth, D. Bosbach, *Chem. Geol.* **2016**, *424*, 51.
[69] J. Weber, J. Barthel, M. Klinkenberg, D. Bosbach, M. Kruth, F. Brandt, *Chem. Geol.* **2017**, *466*, 722.
[70] D. A. Kulik, T. Wagner, S. V. Dmytrieva, G. Kosakowski, F. F. Hingerl, K. V. Chudnenko, U. R. Berner, *Comput. Geosci.* **2013**, *17*, 1.
[71] U. Berner, *Solubility of Radionuclides in a Bentonite Environment for Provisional Safety Analyses for SGT-E2, NAGRA-NTB 14-06*, Nagra, Wettingen, Switzerland **2014**.
[72] SKB, *Data Report for the Safety Assessment SR-Site. Technical Report TR-10-52*, Svensk Kärnbränslehantering AB, Stockholm, Sweden **2010**.
[73] P. Wersin, M. Kiczka, D. Rosch, *Safety Case for the Disposal of Spent Nuclear Fuel at Olkiluoto—Radionuclide Solubility Limits and Migration Parameters for the Canister and Buffer, Posiva Report 2012-39*, Posiva, Eurajoki, Finland **2012**.
[74] P. Wersin, M. Kiczka, D. Rosch, M. Ochs, D. Trudel, *Safety Case for the Disposal of Spent Nuclear Fuel at Olkiluoto—Radionuclide Solubility Limits and Migration Parameters for the Backfill, Posiva Report 2012-40*, Posiva, Eurajoki **2012**.
[75] M. Klinkenberg, J. Weber, J. Barthel, V. Vinograd, J. Poonoosamy, M. Kruth, D. Bosbach, F. Brandt, *Chem. Geol.* **2018**, *497*, 1.
[76] F. Brandt, M. Klinkenberg, J. Poonoosamy, J. Weber, D. Bosbach, *Minerals* **2018**, *8*, 502.
[77] F. P. Glasser, *Mineral. Mag.* **2001**, *65*, 621.
[78] F. P. Glasser, *Handbook of Advanced Radioactive Waste Conditioning Technologies* (Ed: M. I. Ojovan), Woodhead Publishing, Cambridge, UK **2011**, p. 67.
[79] C. Jantzen, A. Johnson, D. Read, J. Stegemann, *Adv. Cem. Res.* **2010**, *22*, 225.
[80] B. Grambow, *Elements* **2006**, *2*, 357.
[81] W. E. Lee, M. I. Ojovan, M. C. Stennett, N. C. Hyatt, *Adv. Appl. Ceram.* **2006**, *105*, 1.
[82] I. W. Donald, *Glass Technol. Eur. J. Glass Sci. Technol.* **2007**, *48*, 155.
[83] I. W. Donald, *Waste Immobilization in Glass and Ceramic Based Hosts*, Wiley, Chichester, UK **2010**.
[84] R. C. Ewing, *Proc. Natl. Acad. Sci. USA* **1999**, *96*, 3432.
[85] R. C. Ewing, *Prog. Nucl. Energy* **2007**, *49*, 635.
[86] R. C. Ewing, L. Wang, *Rev. Mineral. Geochem.* **2002**, *48*, 673.
[87] R. C. Ewing, W. J. Weber, *The Chemistry of the Actinide and Transactinide Elements* (Eds: L. R. Morss, N. M. Edelstein, J. Fuger), Springer, Dordrecht, The Netherlands **2011**, p. 3813.
[88] R. C. Ewing, W. J. Weber, J. Lian, *Appl. Phys. Rev.* **2004**, *95*, 5949.
[89] N. Dacheux, N. Clavier, R. Podor, *Am. Mineral.* **2013**, *98*, 833.
[90] G. Deissmann, S. Neumeier, G. Modolo, D. Bosbach, *Mineral. Mag.* **2012**, *76*, 2911.
[91] G. R. Lumpkin, *Elements* **2006**, *2*, 365.
[92] S. Neumeier, Y. Arinicheva, Y. Ji, J. M. Heuser, P. M. Kowalski, P. Kegler, H. Schlenz, D. Bosbach, G. Deissmann, *Radiochim. Acta* **2017**, *105*, 961.
[93] E. Oelkers, J. M. Montel., *Elements* **2008**, *4*, 113.
[94] A. E. Ringwood, S. E. Kesson, N. G. Ware, W. Hibberson, A. Major, *Nature* **1979**, *278*, 219.
[95] A. E. Ringwood, S. E. Kesson, K. D. Reeve, D. M. Levins, E. J. Ramm, *Radioactive Waste Forms for the Future* (Eds: W. Lutze, R. C. Ewing), North-Holland, Amsterdam, The Netherlands **1988**, p. 233.
[96] S. V. Stefanovsky, S. V. Yudintsev, R. Gieré, G. R. Lumpkin, *Energy, Waste, and the Environment: A Geochemical Perspective* (Eds: R. Gieré, P. Stille) Geological Society, London **2004**, p. 37.
[97] W. J. Weber, A. Navrotsky, S. Stefanovsky, E. R. Vance, E. Vernaz, *MRS Bull.* **2009**, *34*, 46.
[98] K. Holliday, S. Finkeldei, S. Neumeier, C. Walther, D. Bosbach, T. Stumpf, *J. Nucl. Mater.* **2013**, *433*, 479.
[99] B. Klobes, S. Finkeldei, W. Röhrig, D. Bosbach, R. P. Hermann, *J. Phys. Chem. Solids* **2015**, *79*, 43.
[100] B. Klobes, S. Finkeldei, F. Brandt, D. Bosbach, D. Bessas, J. P. Embs, R. Hermann, *Phys. Status Solidi B* **2015**, *252*, 1940.
[101] S. Finkeldei, M. Stennett, P. M. Kowalski, Y. Ji, E. de Visser-Týnová, N. Hyatt, D. Bosbach, F. Brandt, *J. Mater. Chem. A* **2019**, *8*, 2387.
[102] J. Shamblin, M. Feygenson, J. Neuefeind, C. L. Tracy, F. Zhang, S. Finkeldei, D. Bosbach, H. Zhou, R. C. Ewing, M. Lang, *Nat. Mater.* **2016**, *15*, 507.
[103] Y. Li, P. M. Kowalski, G. Beridze, A. Blanca-Romero, Y Ji, V. L. Vinograd, J. Gale, D. Bosbach, *Ceram. Trans.* **2016**, *255*, 165.
[104] P. S. Maram, S. V. Ushakov, R. J. K. Weber, C. J. Benmore, A. Navrotsky, *Sci. Rep.* **2018**, *8*, 10658.
[105] Y. Li, P. M. Kowalski, *J. Nucl. Mater.* **2018**, *505*, 255.
[106] S. Finkeldei, F. Brandt, K. Rozov, A. A. Bukaemskiy, S. Neumeier, D. Bosbach, *Appl. Geochem.* **2014**, *49*, 31.
[107] S. Finkeldei, F. Brandt, A. Bukaemskiy, S. Neumeier, G. Modolo, D. Bosbach, *Prog. Nucl. Energy* **2014**, *72*, 130.
[108] C. Fischer, S. Finkeldei, F. Brandt, D. Bosbach, A. Luttge, *ACS Appl. Mater. Interfaces* **2015**, *7*, 17857.
[109] S. Szenknect, S. Finkeldei, F. Brandt, J. Ravaux, M. Odorico, R. Podor, J. Lautru, N. Dacheux, D. Bosbach, *J. Nucl. Mater.* **2017**, *496*, 97.